Sources of Error in Thermoluminescence Studies

By Jesse M. McNellis

STATE
GEOLOGICAL
SURVEY
OF
KANSAS

BULLETIN 165, PART 2

THE UNIVERSITY OF KANSAS
LAWRENCE, KANSAS - 1963

STATE OF KANSAS ..... John Anderson, Jr., Governor

BOARD OF REGENTS ..... Henry A. Bubb, Chairman
William F. Danenbarger, Vice-Chairman

Whitley Austin	Ray Evans	Dwight D. Klinger
A. H. Cromb	Clement H. Hall	L. M. Morgan
		Clyde M. Reed, Jr.

Max Bickford, Executive Director

MINERAL INDUSTRIES COUNCIL

Howard Carey, Jr.	O. S. Fent	George K. Mackie, Jr.
Simeon S. Clarke	Bruce G. Gleissner	W. L. Stryker
Charles Cook	Dane Hansen	Robert F. Walters
Lee H. Cornell	Beatrice L. Jacquart	Benjamin O. Weaver

STATE GEOLOGICAL SURVEY OF KANSAS

W. Clarke Wescoe, M.D., Chancellor of The University and ex officio Director of the Survey

Frank C. Foley, Ph.D., State Geologist and Director

William W. Hambleton, Ph.D., Assoc. State Geologist and Assoc. Director

Raymond C. Moore, Ph.D., Sc.D., Principal Geologist Emeritus

John M. Jewett, Ph.D., Senior Geologist

Doris E. Nodine Zeller, Ph.D., Editor

Grace E. Muilenburg, B.S., Public Information Director

Kenneth J. Badger, B.A., Chief Draftsman

Lila M. Watkins, Secretary

Research Divisions	Division Head
Basic Geology	Daniel F. Merriam, Ph.D.
Petrography	Ada Swineford, Ph.D.
Geochemistry	Frederic R. Siegel, Ph.D.
Mineral Resources	Allison L. Hornbaker, M.S.
Oil and Gas	Edwin D. Goebel, M.S.
Ceramics	Norman Plummer, A.B.

Cooperative Studies with United States Geological Survey

Ground-Water Resources	Robert J. Dingman, B.S., District Geologist
Minerals Fuels	W. L. Adkison, B.S., geologist in charge

Branch Offices

Geological Survey Well Sample Library, 4150 Monroe, Wichita

Geological Survey Southwest Kansas Field Office, 310 N. 9th Street, Garden City

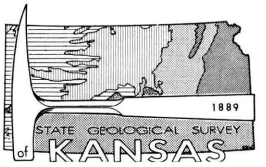

BULLETIN 165, PART 2

Sources of Error in Thermoluminescence Studies

By Jesse M. McNellis

Printed by authority of the State of Kansas
Distributed from Lawrence

UNIVERSITY OF KANSAS PUBLICATIONS
DECEMBER 1963

CONTENTS

ILLUSTRATIONS

TABLES

JESSE M. McNELLIS

Sources of Error in Thermoluminescence Studies[1]

ABSTRACT

Controlled sampling techniques were applied to a small block of limestone from which solid samples and three grain-size fractions were examined. Data from artificial and natural glow curves were analyzed graphically and statistically.

The most satisfactory grain size for future thermoluminescence studies was found to range from 74 to 125 microns. Significantly more thermoluminescence was obtained from samples heated in a nitrogen atmosphere because the filtering effect of oxidized iron was eliminated. After elimination of the filtering effect, iron still inhibited thermoluminescence. The reliability of the nitrogen atmosphere glow curves was approximately equal to that of the normal atmosphere glow curves. Lateral and vertical variations exist in the limestone within short distances and are thought to be dependent primarily upon the trace element content of the material examined.

RESUMEN

Técnicas controladas para obtener muestras fueron aplicadas a un pequeño bloque de caliza, de el cual meustras sólidas y tres muestras de dimensión de grano fueron examinadas. Datos obtenidos de curvas de incandescencia natural y artificial fueron analizados gráficamente y estadísticamente.

La dimensión de grano más satisfactoria para futuros estudios en termoluminiscencia fué encontrada que yace entre 74 y 125 micrones. Significativemente más termoluminiscencia fué obtenida de muestras calentadas en una atmósfera de nitrógeno debido a que el efecto filtrante de hierro oxidado fué eliminado. El hierro inhibió la termoluminiscencia aun después de la eliminación del efecto filtrante.

La veracidad des las curvas de incandescencia en la atmósfera de notrógeno fué aproximadamente igual a la de las curvas de incandescencia en la atmósfera normal. Variaciones laterales y verticales existen en la caliza en breves distancias, y se cree que se deban primeramente a la distribución de los elementos de trazo en el material examinado.

ZUSAMMENFASSUNG

Kontrollierte Probenmethoden wurden an einem kleinen Block Kalkstein angewandt, von dem feste Proben und drei korngrosse Fraktinen geprüft wurden. Die Daten von künstlichen und natürlichen Glow-Kurven wurden graphisch und statistisch ausgewertet.

Dabei fand man, dass die beste Korngrösse für künftige Thermolumineszenzuntersuchungen zwischen 74 und 125 Mikron liegt. Erheblich starkere Thermolumineszenz wurde von Proben erhalten, die in einer Stickstoff-Atmosphäre erhitzt wurden, da dadurch der Filter-Effekt oxidierten Eisens ausgeschaltet wurde. Eisen behinderte die Thermolumineszenz jedoch auch dann noch, als der Filter-Effekt eliminiert worden war. Die Zuverlässigkeit der Glow-Kurven in Stickstoff-Atmosphäre entsprach ungefähr der von Glow-Kurven in normaler Atmosphäre. Laterale und vertikale Variationen existieren im Kalkstein innerhalb kurzer Entfernungen; es wird angenommen, dass sie erster Linie vom Spurenelement-Gehalt des geprüften Materials abhängen.

RÉSUMÉ

On a appliqué des techniques contrôlees d'échantillonnage à un petit bloc de pierre calcaire delaquelle on a examiné des échantillons solides et des fractions d'une grandeur de trois grains. On a analysé graphiquement et statistiquement les données des courbes à incandescence artificielles et naturelles.

On a trouvé que la grandeur de grain la plus satisfaisante pour des études futures de thermoluminescence varie de 74 à 125 microns. On a obtenu beaucoup plus de thermoluminescence des échantillons qui étaient chauffés dans une atmosphère nitrogène parceque, l'effet de filtrage était éliminé. Après l'élimination de l'effet de filtrage, le fer empêchait encore la thermoluminescence. La sécurité des courbes à incandescence de l'atmosphère nitrogène était approximativement égale à celle des courbes à incandescene de l'atmosphère normale. Des variations latérales et verticales existant dans la pierre calcaire en distances brièves et on les croit dépendre surtout de la teneur de l'élément de trace du matériaux examiné.

[1] Based on a thesis submitted in partial fulfillment of the Masters Degree in Geology, University of Kansas, 1959.

INTRODUCTION

Purpose of Investigation

Continued progress in the development of thermoluminescence as a practical geological tool requires recognition and minimization of sources of error. Most previous studies of thermoluminescence have included discussions of sources of error: physical, chemical, and radioactive variations within the material of the sample, and procedural and sampling techniques.

The purpose of this study was two-fold: to point out some of the variables inherent in the material sampled, and to determine the effects of solid samples, different grain-size samples, and nitrogen atmosphere on thermoluminescence.

Acknowledgments

My sincere thanks go to E. J. Zeller, Department of Geology, The University of Kansas, for his suggestions, assistance, and criticisms. I am grateful to Continental Oil Company for making gamma irradiations, to E. E. Angino and W. C. Pearn for their suggestions with regard to the analyses of the collected data, to Walter E. Hill, Jr., and Anna Reid for their laboratory assistance, and to Kenneth O. Mears for his assistance in the collection of the limestone. My wife, Frances, was of great assistance in the preparation of the manuscript.

THERMOLUMINESCENCE

General Theory

Crystalline solids, including many rocks, minerals, and other substances, emit visible light when heated to temperatures below incandescence. This phenomenon is called thermoluminescence.

Normal orbital electrons of crystalline solids possess certain potential energies, which fall within a band or range of energy values known as the ground state. If additional energy is received by electrons in the ground state, these electrons may be raised to the conduction band at a higher energy level than the ground state. When electrons reach the conduction band they may wander through the crystal. As excess energy is dissipated, electrons in the conduction band will either return to the ground state or they will be trapped in areas of the crystal having unsatisfied charges. Trapped electrons possess higher potential energies than those in the ground state. When the crystal is heated the trapped electrons are liberated and return to the conduction band. From the conduction band they may return to the ground state, a process which involves the release of energy in the form of heat and light. Visible light released in this way is thermoluminescence.

Energy necessary to move the electrons from the ground state to the conduction band may be supplied by radioactivity, pressure, or crystallization. Zeller (1953, 1954a, 1954b), and Zeller and others (1955) have discussed in detail these different activators of thermoluminescence.

Measurement

Quantitative measurement of the light emitted when a sample is heated is recorded in the form of a glow curve—a graph of the light emitted plotted against the temperatures applied to the sample. Glow curves normally show one or more peaks which are expressions of maximum light emission at particular temperatures. Radiation-induced thermoluminescence, the type investigated in this study, produces "artificial" or "natural" glow curves depending on whether the energy of electron displacement from the ground state to a trap is supplied artificially or naturally. Samples that are artificially irradiated and are refrigerated until used produce the greater number of peaks.

Application to Geology

The two applications of thermoluminescence to geology that have received the greatest attention have been correlation (Bergstrom, 1956; Parks, 1953; Pitrat, 1956; Saunders, 1953) and age determination (Angino, 1958, 1959; Pearn, 1959; Zeller, 1954a, 1954b; Zeller and Ronca, 1962; Zeller and others, 1957).

MATERIAL USED IN INVESTIGATION

Samples used in this study were collected from the Farley Limestone Member of the Wyandotte Limestone (Pennsylvanian) at an abandoned quarry ¼ mile northeast of Bonner Springs, in the NE NE SE sec. 29, T. 11 S., R. 23 E., Wyandotte County, Kansas. The Farley is an extremely variable sequence of limestone and shale beds. At the locality sampled the Farley consists of limestone beds separated by shale partings at the base, shale with limestone in the middle part, and limestone beds at

the top. The bed sampled is next above the bottom bed of the Farley (Fig. 1). Microscopic examination of the sampled limestone showed it to be a calcarenite containing many macrofossil fragments (mostly molluscs).

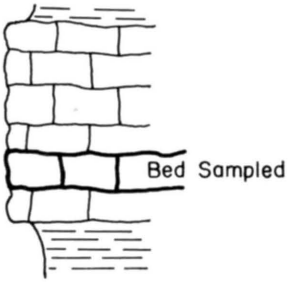

FIGURE 1.—Outcrop position of sampled bed in Farley Limestone.

SAMPLE PREPARATION

From a block of limestone 18 inches long, 8 inches wide, and 7 inches thick, 30 cores averaging 2¼ inches in length by ½ inch in diameter were taken with a drill press and diamond core-drill.

The block was arbitrarily divided into 15 pairs of adjacent cores (Pl. 1). The cores were sawed in half. In each core pair the top half of one core was crushed and the bottom half of the core was sawed into disks; the top half of the adjacent core was sawed into disks and the bottom half of the core was crushed (Fig. 2). The disks of core were ground and polished to a thickness of 1/16 to 1/32 inch. The crushed part of each core was prepared using a steel mortar and pestle for preliminary crushing and a porcelain mortar and pestle for final pulverization. The pulverized sample was passed between the poles of a magnet to remove the iron particles introduced by the crushing process. Using U. S. Standard sieves, each pulverized sample was divided into three fractions. A coarse fraction, *a*, included the particles that passed through the 80-mesh sieve (177-micron openings) and remained on the 100-mesh sieve

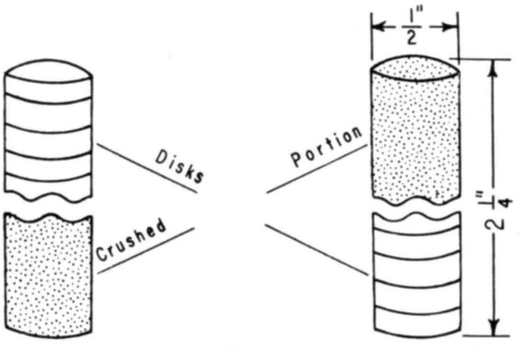

FIGURE 2.—Relative position of samples prepared from each core pair.

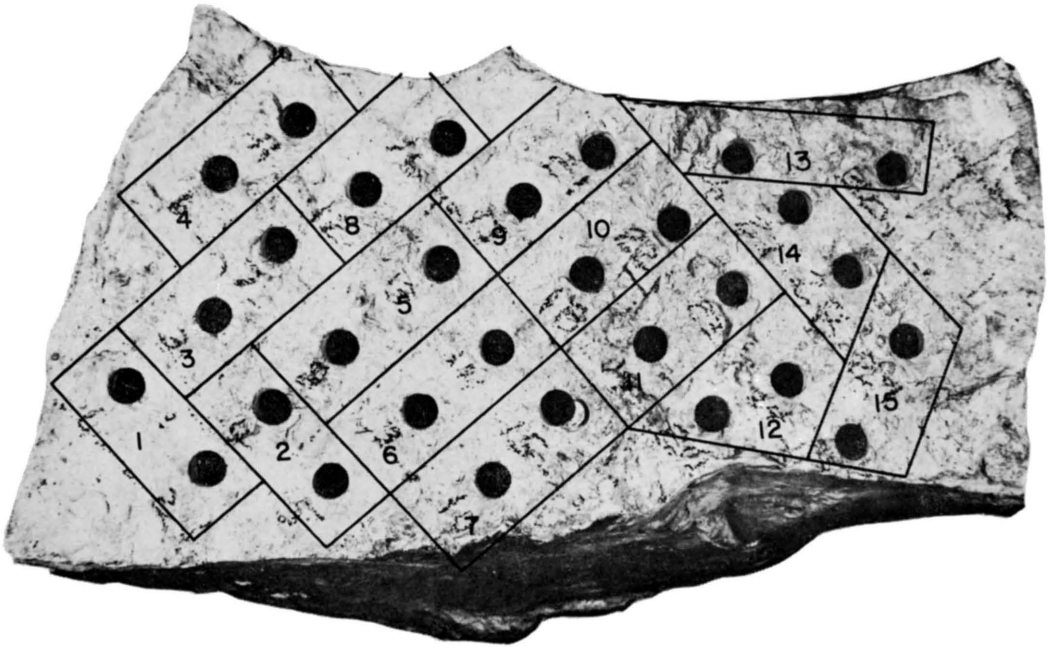

PLATE 1.—Block of limestone used in this investigation, showing arrangement of cores in pairs, numbered as referred to in this report.

(149 microns). An intermediate fraction, *b*, included the particles that passed through the 120-mesh sieve (125 microns) and remained on the 200-mesh sieve (74 microns). The fine fraction, *c*, included the particles that passed through the 200-mesh sieve.

Sample Irradiation

The samples were artificially irradiated to obtain the maximum number of glow curve peaks. The three crushed fractions, packaged in gelatin capsules, and the solid disks were irradiated at the Continental Oil Company laboratory in Ponca City, Oklahoma. Spent fuel rods from an atomic pile were employed as the source of gamma radiation.

After irradiation the samples were kept refrigerated until glow curves were run.

Unfortunately, not all samples received the same radiation dosage. The coarse or *a* fraction received the maximum dosage; the intermediate or *b* fraction, part of the fine or *c* fraction, and all disks received the intermediate dosage; the remainder of the fine fraction received the minimum dosage. The different radiation dosages were not given in roentgens but in milliamperes as measured by an ionization chamber. The milliampere readings were used to equate the three radiation dosages (Appendix A).

GRAPHIC AND STATISTICAL ANALYSES

Glow Curve Data

Artificial glow curves were run under a normal atmosphere and under a nitrogen atmosphere. In addition, natural glow curves were run under a normal atmosphere.

All artificial glow curves had a low-temperature peak at approximately 110°C, a high-temperature peak at approximately 300°C, and one or both of two peaks at approximately 180°C and 235°C. For purposes of this discussion the normal atmosphere glow curve peaks are numbered 1 through 4, in the order of increased temperature, and the nitrogen atmosphere peaks 1N through 4N. The high-temperature peak at approximately 325°C, designated 4u, was the only significant peak in the natural glow curves. Typical artificial and natural glow curves are illustrated in Figure 3.

Variations in the thermoluminescence of the samples required use of different amplifications on the glow curve assembly. Measurements of the heights of peaks in centimeters were equated using the proper amplification factors. The equated peak heights were graphed, and these values were analyzed statistically. The peak values are listed in Appendices E (normal atmosphere artificial glow curves), F (nitrogen atmosphere artificial glow curves), and G (normal atmosphere natural glow curves).

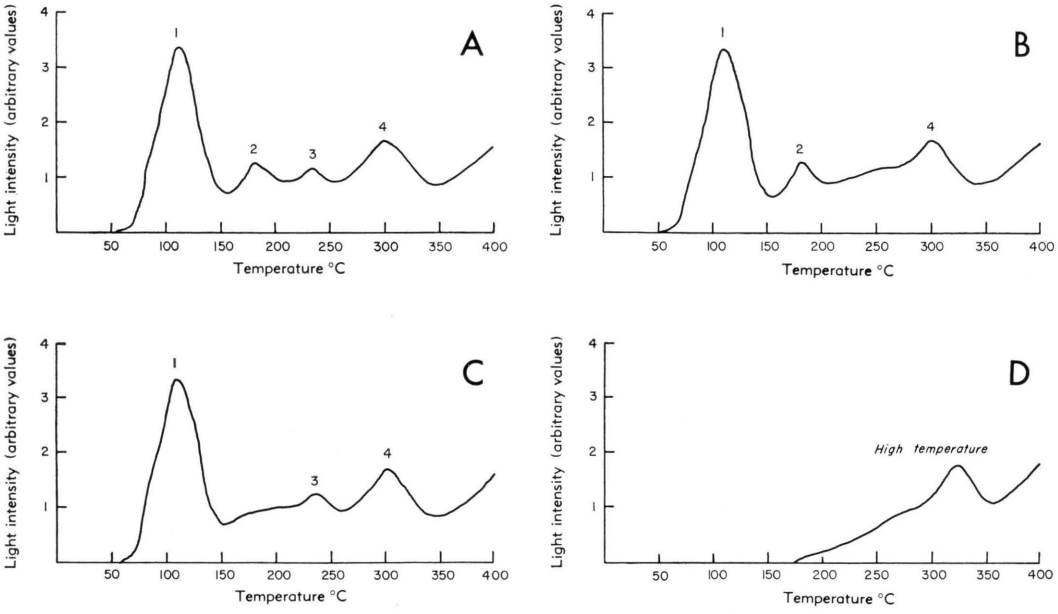

Figure 3.—Examples of glow curves obtained in investigation. **A, B,** and **C,** artificial glow curves showing peaks 1, 2, 3, and 4. **D,** natural glow curve showing high-temperature peak.

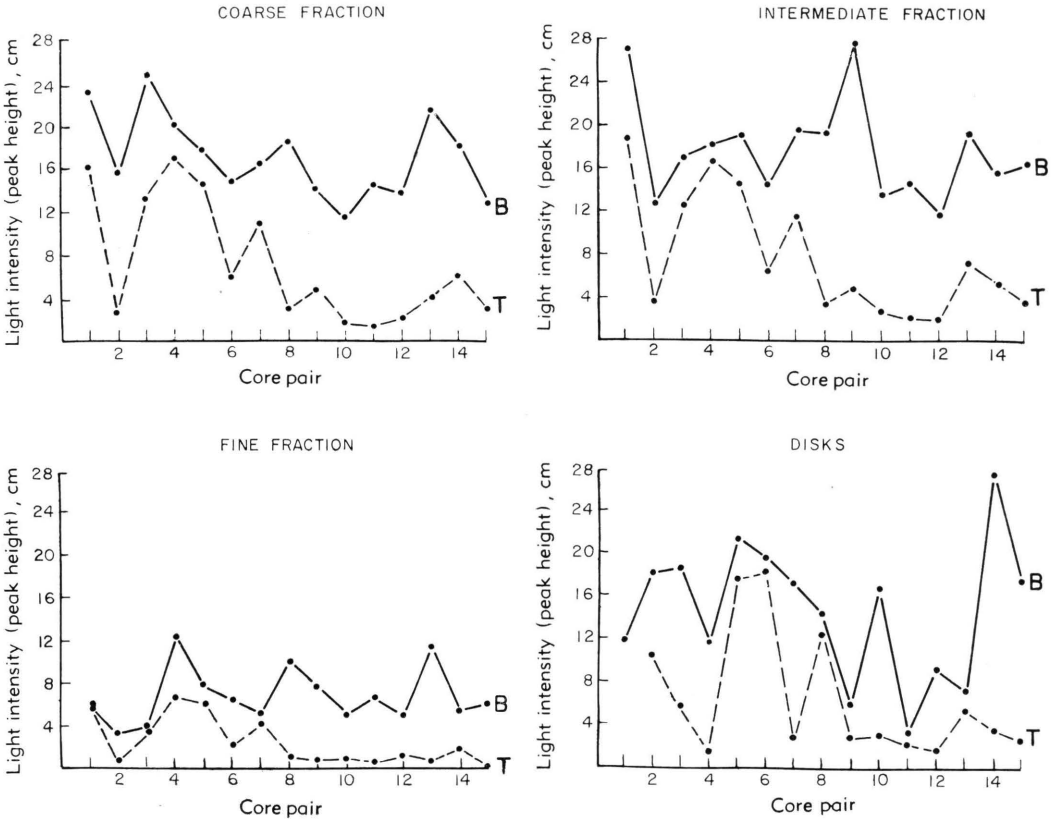

FIGURE 4.—Peak 1 vertical variation comparison graphs. T indicates core tops; B, core bottoms.

Normal Atmosphere Artificial Glow Curves

PEAK 1

The values of peak 1 for the tops and bottoms of cores of each fraction in each core pair were plotted. The resulting graphs illustrate the variation in thermoluminescence between the tops and the bottoms of adjacent cores (Fig. 4).

The coarse and intermediate fractions of core bottoms are almost equal in total thermoluminescence (Fig. 5), and the same is true of

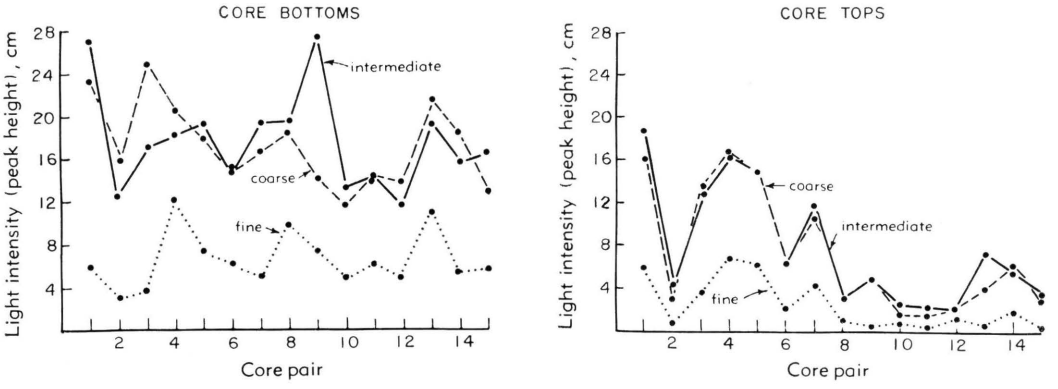

FIGURE 5.—Peak 1 bottom and top comparison graphs.

core tops. The fine fraction produced the lowest values of thermoluminescence.

TABLE 1.—Results of statistical analysis of peak 1 values.

Fraction	Mean	Standard deviation	Percent deviation	T/B[a] percentage
a[b] T	7.32	5.45	74.5	42.2
a B	17.34	3.79	21.9	
b T	7.74	5.49	70.9	43.3
b B	17.86	4.5	25.2	
c T	2.49	2.18	87.6	36.8
c B	6.76	2.55	37.7	
d T	6.37	5.54	87.0	44.1
d B	14.44	6.32	43.8	

[a] T, core top; B, core bottom. Used in all subsequent tables and the Appendices.
[b] *a*, coarse fraction; *b*, intermediate fraction; *c*, fine fraction; *d*, disks. Used in all subsequent tables and in the Appendices.

The results of the statistical analysis of peak 1 values are listed in Table 1. The mean is a function of the total thermoluminescence. The values of the means of the tops for all size fractions and the disks average 41.6 percent of the values for the bottoms. The means of the various fractions demonstrate that the intermediate-size or *b* fraction gives the greatest amount of thermoluminescence and that the fine or *c* fraction gives the least. The coarse and intermediate fractions, having the lowest percentages of deviation, are comparable and give the most consistent results. The disks have values of thermoluminescence between those of the coarse and fine fractions, and their standard deviation and percent of deviation is high.

Vertical variation is verified by the T(top)/B(bottom) ratio. Lateral variation is not as simply presented. The difficulty in presentation was overcome by dividing the block into five divisions (Pl. 2). Mean values of peak 1 heights of the intermediate fraction were then plotted for the core tops and bottoms of each division. (The intermediate fraction also is used in all subsequent lateral variation graphs of glow-curve data.) (Fig. 6.)

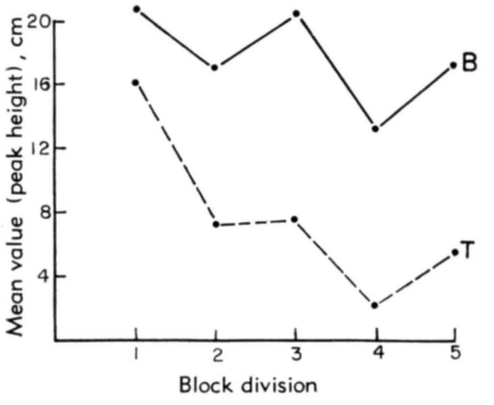

FIGURE 6.—Peak 1 lateral variation comparison graph.

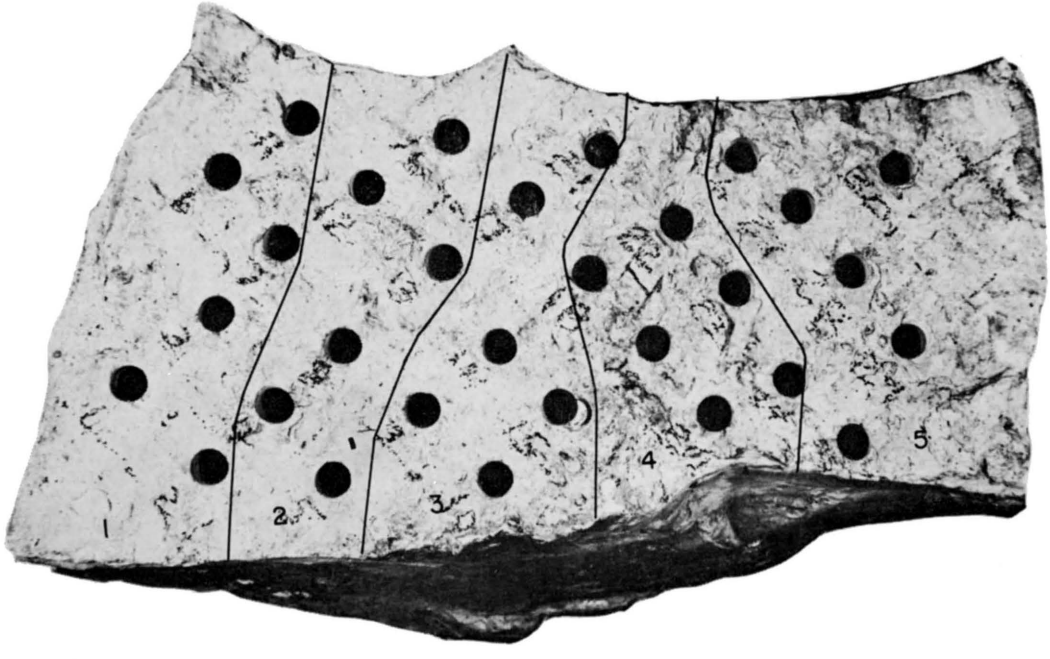

PLATE 2.—Cored block of limestone showing the lateral block divisions used in investigation of lateral variation.

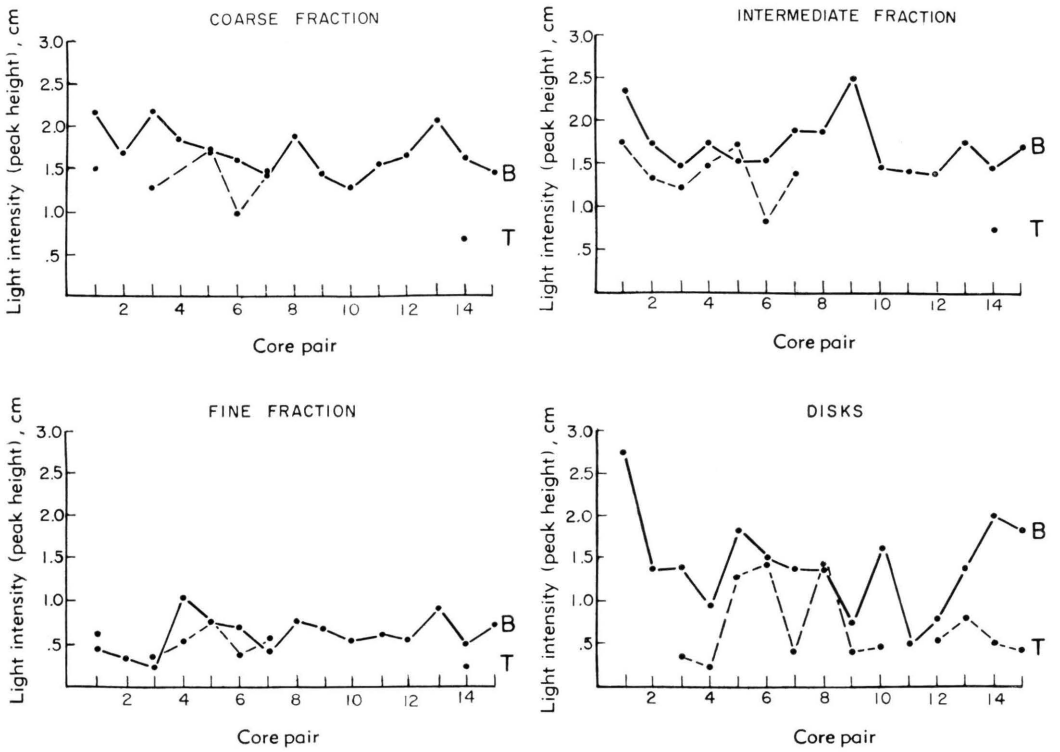

FIGURE 7.—Peak 2 vertical variation comparison graphs.

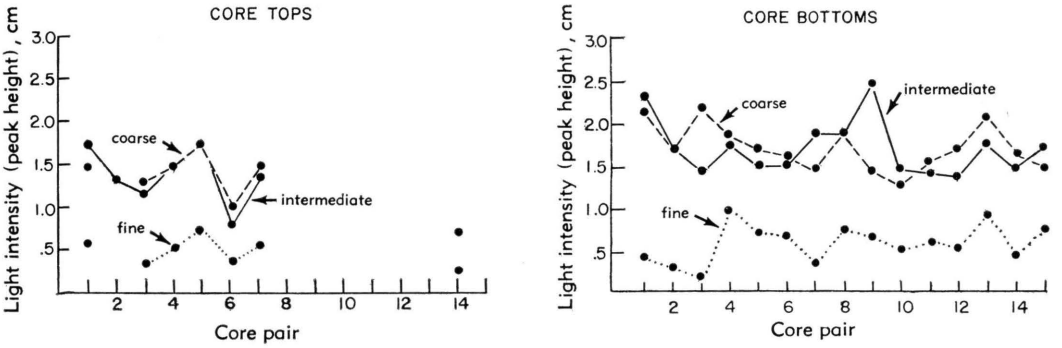

FIGURE 8.—Peak 2 bottom and top comparison graphs.

PEAK 2

This peak was not present, for measurable purposes, in all core tops. It was present, however, in all core bottoms. Graphs for the various fractions and the disks were made (Fig. 7, 8). Vertical variation between tops and bottoms of cores is illustrated; the coarse and intermediate fractions have almost equal values of thermoluminescence, and the fine fractions have the lowest values.

The results of the statistical analysis are shown in Table 2. The tops of the cores do not

TABLE 2.—Results of statistical analysis of peak 2 values.

Fraction	Mean	Standard deviation	Percent deviation	T/B percentage
a T	1.27	.425	33.5	75.1
a B	1.69	.277	16.5	
b T	1.31	.332	25.4	77.0
b B	1.70	.239	14.1	
c T	.44	.163	37.0	73.3
c B	.60	.242	40.3	
d T	.85	.681	80.1	61.2
d B	1.39	.501	31.0	

show as much thermoluminescence as the core bottoms. The intermediate fraction has the greatest value of thermoluminescence and the least percent of deviation. The fine fraction has the least deviation but its thermoluminescence values are small and its percent of deviation is high. The disks have values of thermoluminescence between those of the fine and intermediate fractions, and their standard deviation and percent of deviation are high.

The lateral variation for peak 2 was computed and plotted as for peak 1 (Fig. 9).

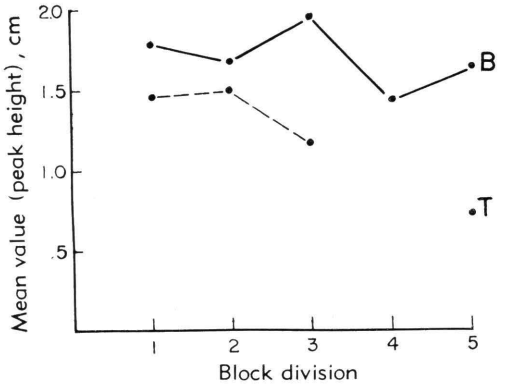

FIGURE 9.—Peak 2 lateral variation comparison graph.

PEAK 3

This peak was measurable in most of the core tops but in only 3 of the core bottoms. A graph of peak 3 values in core top fractions was plotted as for peaks 1 and 2 (Fig. 10). The graph illustrates that the coarse and intermediate fractions give almost equal values of thermoluminescence and that the fine fraction gives the least.

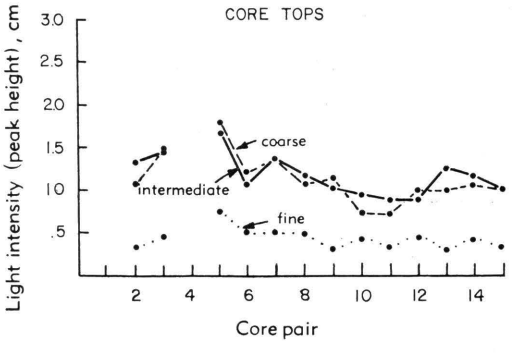

FIGURE 10.—Peak 3 top comparison graph.

TABLE 3.—Results of statistical analysis of peak 3 values.

Fraction	Mean	Standard deviation	Percent deviation
a T	1.14	.285	25.20
b T	1.18	.223	19.0
c T	.41	.211	51.5
d T	.91	.352	38.9

The results of the statistical analysis are listed in Table 3. The intermediate fraction gives the most thermoluminescence with the least percent of deviation; the coarse or *a* fraction thermoluminescence is almost comparable. The fine fraction has the lowest standard deviation, lowest thermoluminescence values and the highest percent of deviation. Again, the disks gave intermediate results.

The lateral variation was computed and plotted as for peaks 1 and 2 (Fig. 11).

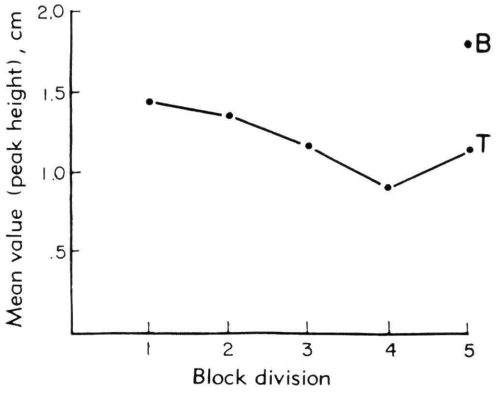

FIGURE 11.—Peak 3 lateral variation graph.

PEAK 4

The peak is present in tops and bottoms of all cores for all fractions and disks. Graphs of the various peak heights were plotted (Fig. 12, 13). Variations between tops and bottoms of cores are apparent. Graphs showing peak heights of the three size fractions show that the fine fraction values for both bottoms and tops of cores are substantially less than the values for the corresponding coarse and intermediate fractions.

The results of the statistical analysis are listed in Table 4. The core top values of thermoluminescence are substantially less than the bottom values. Except for the core bottom values of the coarse fraction, the intermediate fraction produced the maximum thermolumines-

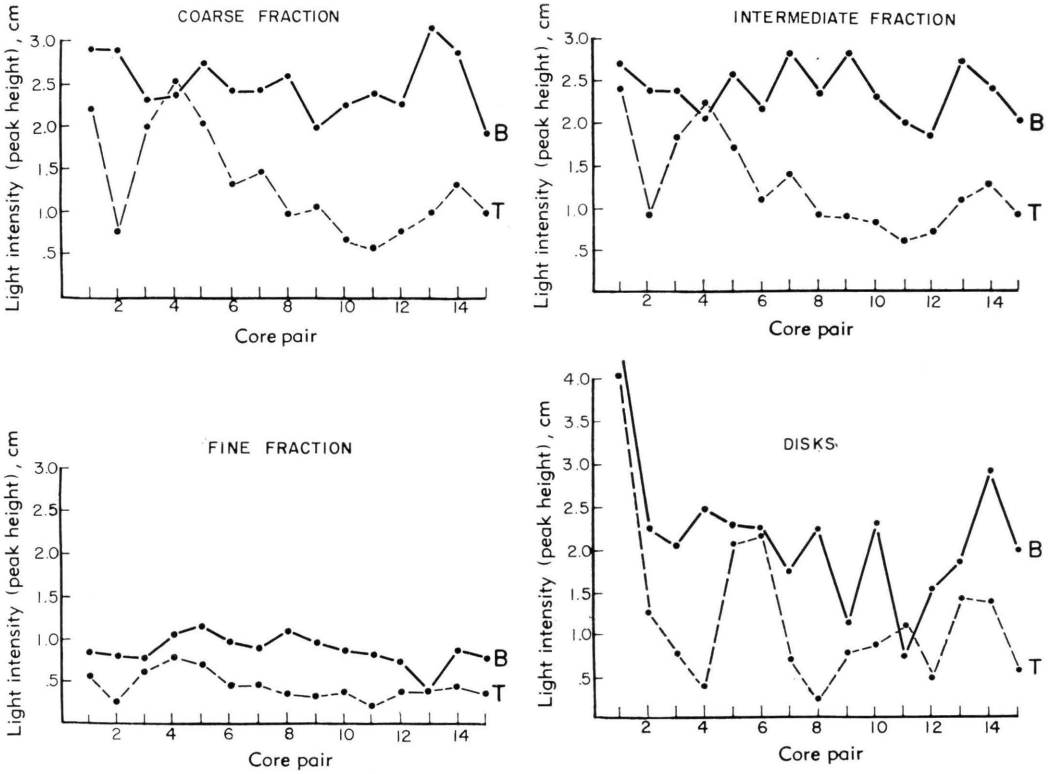

FIGURE 12.—Peak 4 vertical variation comparison graphs.

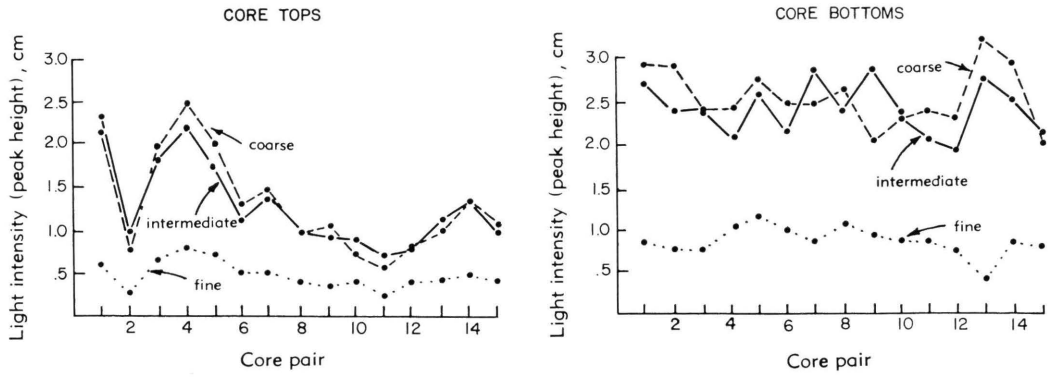

FIGURE 13.—Peak 4 bottom and top comparison graphs.

cence. The core top fine-fraction values have the least deviation and percent of deviation, but the thermoluminescence is quite low. The disks have rather high values of thermoluminescence, but their percent of deviation is also high.

The lateral variation was computed and plotted as for peaks 1, 2, and 3 (Fig. 14).

TABLE 4.—Results of statistical analysis of peak 4 values.

Fraction	Mean	Standard deviation	Percent deviation	T/B percentage
a T	1.31	.586	44.7	51.3
a B	2.55	.395	15.5	
b T	1.37	.521	38.0	57.5
b B	2.38	.30	12.6	
c T	.46	.161	34.9	52.8
c B	.87	.182	20.9	
d T	1.24	.932	75.2	57.4
d B	2.16	.831	38.5	

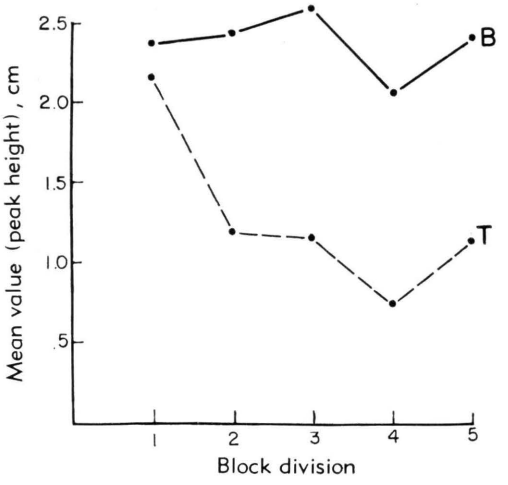

FIGURE 14.—Peak 4 lateral variation comparison graph.

TABLE 5.—Results of statistical analyses of nitrogen atmosphere glow curves, and comparable results of normal atmosphere glow curves.

Peak	Fraction	Mean	Standard deviation	Percent deviation	T/B percentage
1N[a]	*b*N T	4.36	3.33	76.4	37.9
	*b*N B	11.49	3.12	27.2	
1	*b* T	7.74	5.49	70.9	43.3
	b B	17.86	4.5	25.2	
2N	*b*N T	1.49	.416	27.9	74.8
	*b*N B	1.99	.383	19.3	
2	*b* T	1.31	.332	25.4	77.0
	b B	1.70	.239	14.1	
3N	*b*N T	1.3	.242	18.6	
3	*b* T	1.18	.223	19.0	
4N	*b*N T	1.41	.474	33.6	52.6
	*b*N B	2.68	.340	12.7	
4	*b* T	1.37	.521	38.0	57.5
	b B	2.38	.30	12.6	

[a] N indicates nitrogen atmosphere; used also in the Appendices.

Nitrogen Atmosphere Artificial Glow Curves

The nitrogen atmosphere glow curves were run two months after the normal atmosphere glow curves. Measurements in centimeters were made of the heights of peaks 1N, 2N, 3N, and 4N. The statistical analysis of the normal atmosphere artificial glow curve data indicated that the intermediate fraction provided the most thermoluminescence and the most reliable and consistent results; therefore, the intermediate fraction was used for the nitrogen atmosphere glow curves. The peak heights were graphed and statistically analyzed. The results of the statistical analyses of the nitrogen atmosphere glow curves are listed with the corresponding results of the normal atmosphere glow curves for purposes of comparison (Table 5).

PEAK 1N

Comparison with peak 1 values demonstrates a decrease in thermoluminescence as expressed by peak 1N. The percentages of deviation for both peaks are approximately comparable. The percentages of decrease in thermoluminescence from peak 1 to peak 1N are: tops, 43.7 percent; bottoms, 35.7 percent; average, 39.7 percent. Lateral variation graphs were derived following the procedure outlined for normal atmosphere glow curves; peak 1 and peak 1N values appear in Figure 15.

PEAK 2N

Examination of Table 5 demonstrates that peak 2N has a greater value of thermolumines-

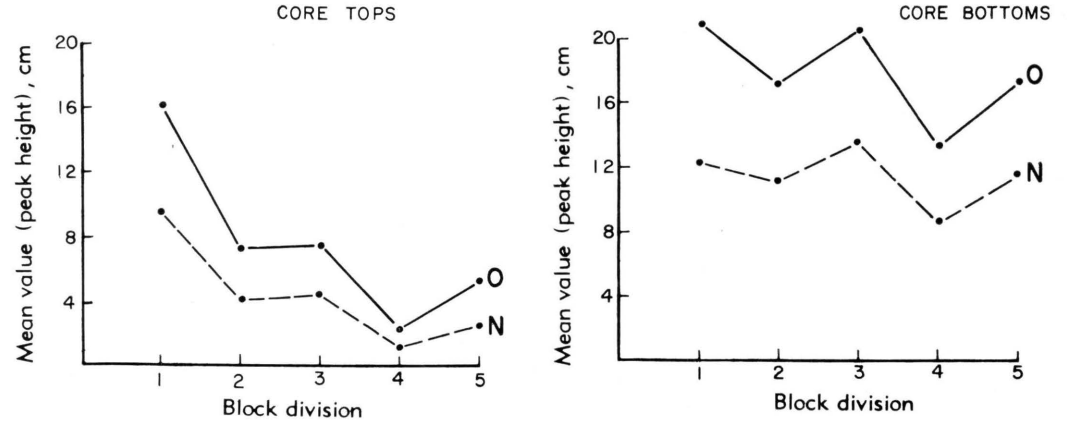

FIGURE 15.—Peak 1N and peak 1 lateral variation comparison graphs. N indicates nitrogen atmosphere; O, normal atmosphere (also used on subsequent figures).

cence than peak 2. The graph of lateral variation illustrates this increase (Fig. 16). The percentages of deviation are approximately equal for tops and bottoms in both peaks. The percentages of increase in thermoluminescence from peak 2 to peak 2N are: tops, 14.6 percent; bottoms, 17.1 percent; average, 15.85 percent.

PEAK 3N

Table 5 demonstrates that peak 3N produced larger values of thermoluminescence than peak 3 and that the percent deviation is almost identical for both peaks. The increase in thermoluminescence from peak 3 to peak 3N is 10.2 percent. The lateral variation graph illustrates this increase (Fig. 17).

PEAK 4N

The percentages of increase in thermoluminescence from peak 4 to peak 4N are: tops, 2.9 percent; bottoms, 12.6 percent; average, 7.75 percent. Peak 4N produced more thermoluminescence than peak 4 and the percentages of deviation for the tops and bottoms of both peaks agree statistically (Table 5). An illustration of the increase in thermoluminescence is provided by the lateral variation graphs (Fig. 18).

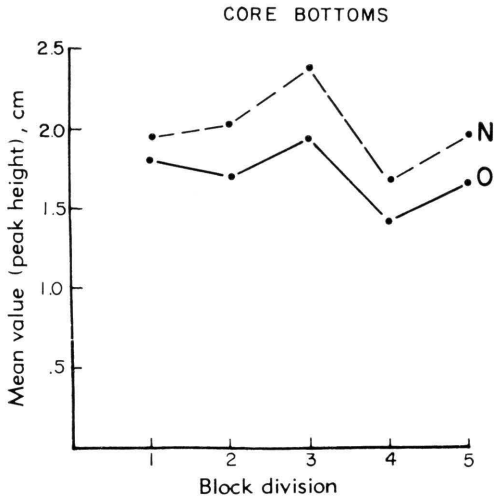

FIGURE 16.—Peak 2N and peak 2 lateral variation comparison graph.

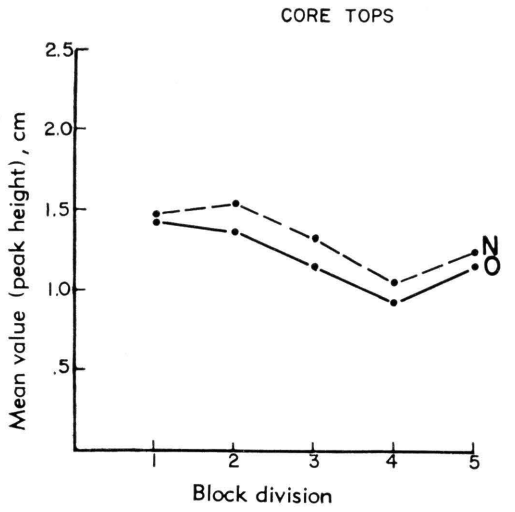

FIGURE 17.—Peak 3N and peak 3 lateral variation comparison graph.

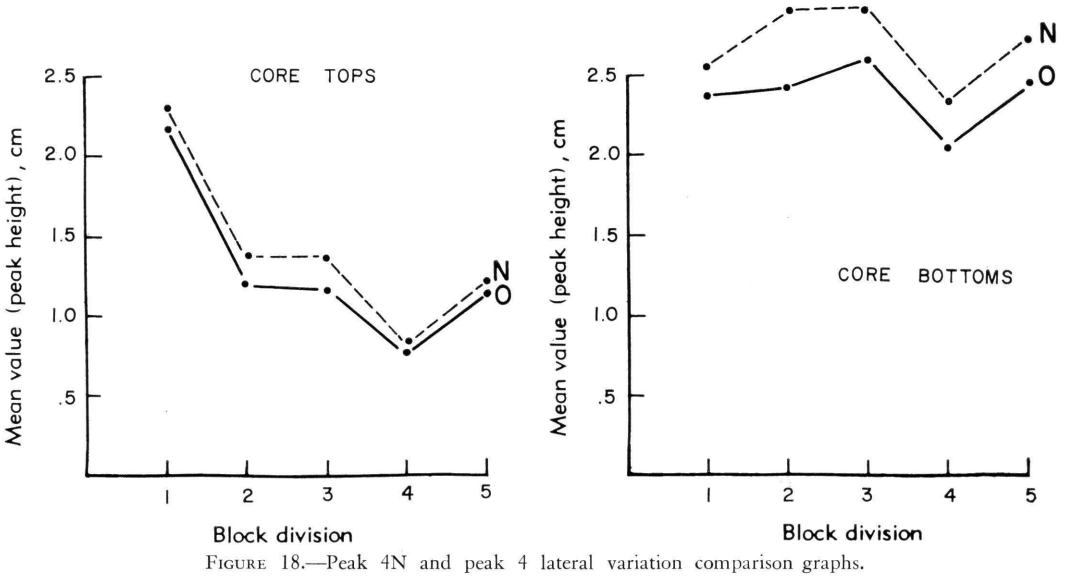

FIGURE 18.—Peak 4N and peak 4 lateral variation comparison graphs.

Normal Atmosphere Natural Glow Curves

The series of natural glow curves was run after the analyses of the artificial glow curves were made. On the basis of the first analyses the intermediate fraction was selected for this series of glow curves.

HIGH-TEMPERATURE PEAK

The high-temperature peak, 4u, is present in the glow curves of the unirradiated intermediate-fraction samples. (An unmeasurable remnant signified the presence of peak 3 in most of the natural runs.) A graph of the peak height values for tops and bottoms of cores (Fig. 19) illustrates that greater thermoluminescence was derived from the bottoms of the cores.

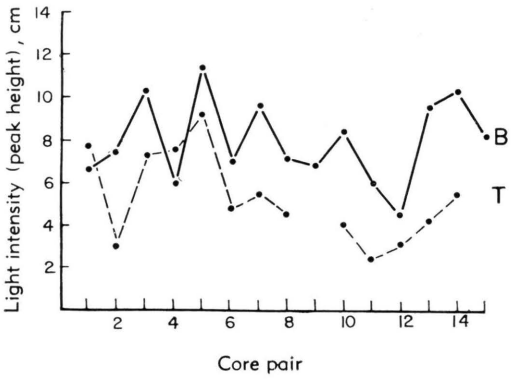

FIGURE 19.—Natural high-temperature peak (4u) vertical variation comparison graph.

Table 6 lists the results of the statistical analysis. The value of thermoluminescence of the tops is 67.1 percent of the value of the bottoms of the cores. Percent deviation for the bottoms of the cores is less than for the tops.

TABLE 6.—Results of statistical analysis of peak 4u values.

Fraction	Mean	Standard deviation	Percent deviation	T/B percentage
*b*u[a] T	5.35	2.03	37.9	67.1
*b*u B	7.97	1.94	24.3	

[a] u indicates natural glow curve; used also in the Appendices.

The lateral variation was computed and plotted following the procedure for peaks of the artificial glow curves (Fig. 20).

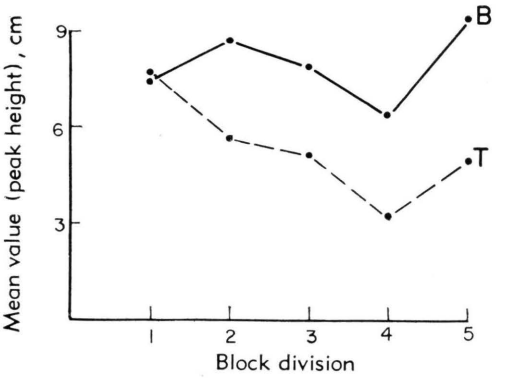

FIGURE 20.—Natural high-temperature peak (4u) lateral variation comparison graph.

IRON, INSOLUBLE RESIDUE, AND TRACE ELEMENT DATA

In an attempt to explain the rather large lateral and vertical variations in thermoluminescence that were found, various laboratory examinations were made. Qualitative trace element analyses were made on samples of 16 cores with a 1.5-meter ARL* grating spectrograph, and an ARL densitometer was used to read the film (Appendix B). Quantitative iron analyses were made using wet chemical methods. Insoluble residues of samples from 16 cores were determined using standard procedures.

Iron content percentages are listed in Appendix C. The values of iron content for the tops and bottoms of cores were plotted for each core pair, and the resulting graph illustrates the variation in iron content between the tops and bottoms of adjacent cores (Fig. 21). The lateral

* Applied Research Laboratories.

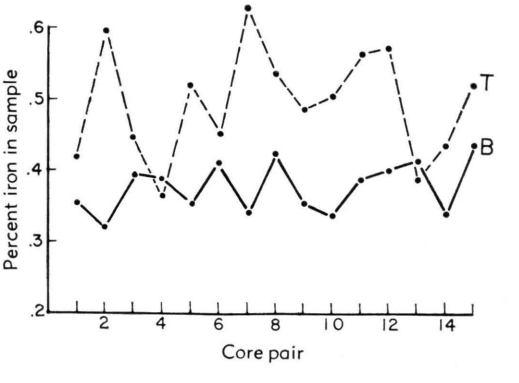

FIGURE 21.—Iron content vertical variation comparison graph.

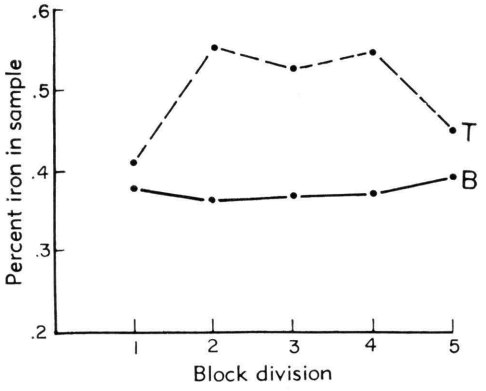

FIGURE 22.—Iron content lateral variation comparison graph.

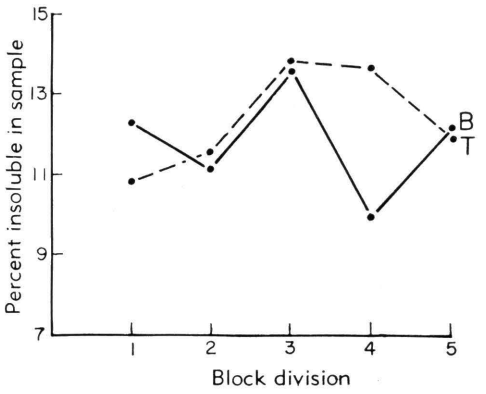

FIGURE 24.—Insoluble residue content lateral variation comparison graph.

variation was computed and plotted as for peak heights (Fig. 22).

The average iron content for samples from the tops of cores was .497 percent; from the bottoms it was .377 percent. For all samples the average was .437 percent. T/B ratio was 127 percent.

Insoluble residue content percentages of the 8 core pairs analyzed are listed in Appendix D. The values of insoluble residue content for the tops and bottoms of cores were plotted, and variation between the tops and bottoms of adjacent cores is illustrated by the resulting graph (Fig. 23). A lateral variation graph also was plotted (Fig. 24).

The average insoluble residue content of samples from the tops of cores was 12.3 percent; from the bottoms it was 11.7 percent. All samples averaged 12 percent. T/B ratio was 105 percent.

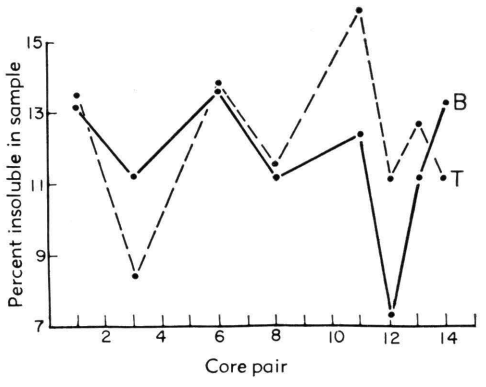

FIGURE 23.—Insoluble residue content vertical variation comparison graph.

Comparison with Glow Curve Data

The lateral variation of iron content, insoluble residue content, and thermoluminescence values are presented graphically (Fig. 25). On all graphs values of all factors increase from right to left. The apparent effect of iron and insolubles on thermoluminescence values of the various peaks is shown. A graph of lateral variation of the T/B ratios of iron, insoluble residue content, and thermoluminescence values of peaks 1, 2, 4, and 4u (Fig. 26) illustrates the systematic variation of iron and insolubles paralleling the variation of thermoluminescence.

SUMMARY

1. The intermediate or *b* fraction (74 to 125 microns) samples had a smaller percent deviation and more thermoluminescence than other crushed fractions.

2. Crushed samples had a smaller percent deviation than solid samples.

3. Peaks 2, 3, and 4 showed an 11 percent average increase in thermoluminescence when run under a nitrogen atmosphere.

4. Peak 1N showed a 40 percent decrease in thermoluminescence from peak 1, which occurred over a two-month period.

5. Large lateral and vertical variations of thermoluminescence existed over extremely short distances in the limestone block sampled.

6. Iron content is related to some of the variations in thermoluminescence.

7. Insoluble residue content may be related to some of the variations in thermoluminescence.

THEORETICAL CONSIDERATION OF RESULTS

Crushed Samples

Intermediate-fraction samples provide the most thermoluminescence and have the lowest percent deviation. Therefore, this fraction is recommended for future thermoluminescence studies.

The coarse fraction was almost as reliable as the intermediate fraction. It is the writer's opinion that the largest particles are the inhibiting factor in coarse-fraction thermoluminescence.

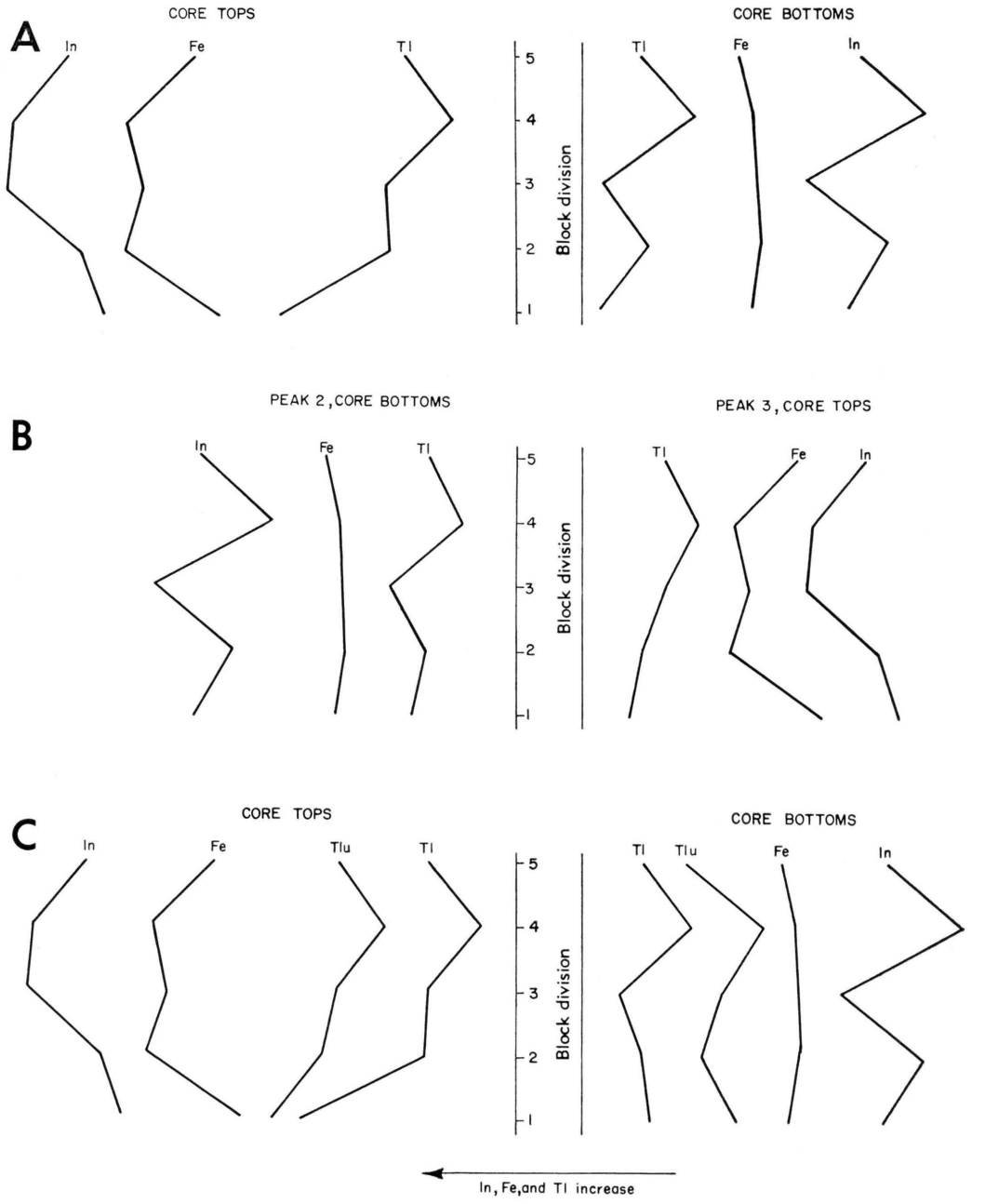

Figure 25.—Lateral variation comparison graphs of insoluble residue (In) content and iron (Fe) content with thermoluminescence (Tl) of **A,** peak 1; **B,** peak 2 and peak 3; and **C,** peak 4 and peak 4u (Tlu).

The 80-mesh size particles are thought to be large enough for excessive decrepitation to occur during the running of a glow curve. This decrepitation could disarrange the sample surface and a subsequent decrease, or in some instances an increase, of thermoluminescence would result. Thus, the coarse fraction would have a slightly larger percent deviation, which is indicated by the greater inconsistency in results.

The fine fraction was consistently lower in total thermoluminescence and the percent deviation was consistently higher than for other fractions. The finer the material the more surface area exposed, which should allow the fine fraction to be the best fraction for thermoluminescence studies. However, this fraction is so fine that its greater number of surface areas serve to increase light scattering. The emitted light is reflected and refracted from crystal surface to crystal surface. Thus, the emitted light from many of the crystal surfaces is effectively masked from measurement. It is thought that the degree of light scattering must vary to an extent great enough to cause the generally large percent deviation observed in the fine fraction results. The coarse and intermediate fractions also scatter the light emitted, but not to the extent that the fine fraction does.

Crushed Versus Solid Samples

Crushed samples show smaller percentages of deviation than solid samples. Individual disks produced large values of thermoluminescence in some instances and small values in other instances. This is thought to be due to the essentially pure calcite which makes up some of the fossil fragments in the limestone. The fossil fragment particles are distributed throughout a crushed limestone sample; but a disk can present a surface that is predominantly fossil fragments (essentially pure calcite), or one that is almost lacking fossil fragments. A disk of either character will not give an average value of thermoluminescence for the material being tested. Crushed samples, because of more random mixing of fossil fragments, provide more uniform results.

Thermoluminescence in Nitrogen Atmosphere

The observed increase in thermoluminescence may be attributed to practical elimination of oxidation of the iron content of the samples through use of a nitrogen atmosphere. Iron oxidation can be observed in samples run under normal atmosphere by a darkening of the sample after temperatures of 150°C are reached. This discoloration decreases the transparency of the sample; in effect, oxidation of iron filters thermoluminescence.

The 11 percent increase in thermoluminescence in peaks 2N, 3N, and 4N effectively increases the sensitivity of the glow curve assembly by that amount. Whether an 11 percent increase in sensitivity would result in all cases would depend on the iron content of the material tested. From this study it appears that an iron content of .377 percent of total sample would make the use of a nitrogen or another inert atmosphere desirable.

The decrease in peak 1N thermoluminescence is the result of the two-month delay in running the nitrogen atmosphere glow curves. A similar decrease in low-temperature peak thermoluminescence was noted by E. E. Angino (personal communication). The decrease apparently results from drainage of electrons in low-temperature traps (Zeller and Ronca, 1962) and is not due to the use of nitrogen. On the basis of the results obtained, it is recommended that glow curves be run as soon as possible after samples are irradiated.

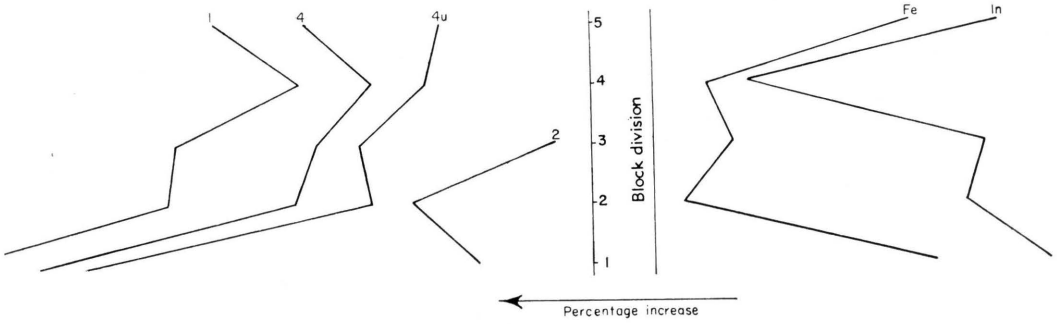

Figure 26.—Lateral variation comparison graph of T/B percentages of iron (Fe), insoluble residue (In), and thermoluminescence values of peaks 1, 2, 4, and 4u.

Vertical and Lateral Variations

Some of the results obtained cannot be explained in light of present knowledge. The order of magnitude of the variation found in this small volume of Farley Limestone is not thought to be the average variation to be found in all limestone. It does demonstrate, however, that high orders of variability can exist in limestone, and future workers should analyze their data with this in mind.

The variation found in this small piece of limestone demonstrates why correlation by thermoluminescence glow curve shape has not been highly successful. Correlation may still be possible if extensive lateral sampling of a horizon at each outcrop is followed by a thorough mixing of the crushed sample. Such a random mixing should give an average thermoluminescence for that horizon at that outcrop. This average thermoluminescence should be much closer to the average thermoluminescence of the same horizon at another locality.

Relation of Iron and Insoluble Residue

The peaks appearing at temperatures above 150°C produced increased values of thermoluminescence on nitrogen atmosphere glow curves. The increase in thermoluminescence allows one to assume that the filtering effects of iron oxidation are practically eliminated. However, the graphs of lateral variation of iron content and of thermoluminescence indicate that iron has a definite inhibiting effect on thermoluminescence after the filtering action of iron oxidation has been practically eliminated.

Inhibition of thermoluminescence due to iron is not pronounced in the bottoms of cores (Fig. 25) but is apparent in the tops of cores. Figure 26 illustrates iron inhibition of thermoluminescence still more decisively for peaks 1, 4, and 4u, but apparently not for peak 2. The absence of peak 3 in bottoms of cores probably is not due to iron inhibition. If the iron content of material used in future thermoluminescence studies varies, a similar variation is to be expected in thermoluminescence values.

The bottoms of cores in Figure 25 illustrate the apparent direct relationship of insoluble residue content to thermoluminescence values. Tops of cores in the same figure show an inverse relationship. This points to the presence of some constituent(s) in core tops (but not bottoms) that inhibits thermoluminescence, or to the presence in core bottoms (but not tops) of a constituent(s) that enhances thermoluminescence. Future control studies must determine what makes up the insoluble residue content of samples in order to determine specific effects of insolubles on thermoluminescence.

Relation of Trace Elements

The trace element analyses indicated that there were seven variable trace elements present in appreciable amounts in the limestone. The variable elements to be considered are Si, Al, Mn, Fe, Mg, V, and Sr. The effects of the iron content were discussed in the preceding section. Some of the variable elements may be part of the insoluble residue content. Pitrat (1956) demonstrated that Mg limestone tends to have a higher second peak which he found at an average temperature of 200° C. This peak lies between peaks 2 and 3 as designated in this study. Medlin (1959) concluded that most of the important thermoluminescence properties of natural calcite samples were due to the presence of divalent Mn, and that Fe, Co, and Ni inhibited thermoluminescence. He found that other impurities were of minor importance.

Examination of the graphs of tops of cores for all peaks shows a striking similarity in their character. Therefore, it appears that whatever is affecting the tops of cores is operating for all peaks. The similarity of the graphs of the bottoms of the cores is not as apparent. Intensive trace element studies should eventually point out the elements or combinations of elements causing some of the variations that occur.

CONCLUSIONS

Future workers making attempts to apply thermoluminescence techniques to geologic problems should strongly consider the effect of grain size on the reproducibility of glow curves. This study indicates that the 74- to 125-micron fraction provides the most reliable and reproducible results.

An increase in thermoluminescence of 11 percent for peaks appearing above temperatures of 150°C resulted from use of a nitrogen atmosphere. This increase is attributed to the practical elimination of the filtering effects of iron oxidation. No appreciable decrease in the reliability or reproducibility of results through use of the nitrogen atmosphere was demonstrated.

Variations within a limestone can be strikingly illustrated by thermoluminescence studies. Some variations can be attributed to the iron content of the material examined. In this study it has been observed that iron acts as an inhibitor of thermoluminescence, particularly for the high- and low-temperature peaks. Future investigators should assume that iron acts as an inhibitor, and as a filter when oxidized. When variations due to other factors are analyzed, thermoluminescence techniques may become increasingly useful in studies of the deposition and sedimentation of limestone, as well as in studies on correlation and age determination.

APPENDICES

A—Equating Radiation Dosages

Sample portion	Radiation dosages, milliamperes	Equating factor
a fraction	79	1
b fraction	72	1.097
c fraction cores (1, 3, 6, 8, 9, 10, 11, 12, 13, 14, 16, 18, 19, 20, 21, 22, 23, 24, 25, 26, 27, 28)	72	1.097
disks	72	1.097
c fraction cores (2, 4, 5, 7, 15, 17, 29, 30)	55	1.437

B—Results of Qualitative Spectrographic Analyses

A semiquantitative analysis was attempted using the results of each sample run. No standards were set up, however, and this analysis proved to be of little value except for its gross aspect. Of the elements listed, Ti, Ag, Cu, and Ca appeared to be constant in amount per sample, while the other seven elements varied from sample to sample. The following cores were analyzed.

Core pair	Core	Core pair	Core
1	1	9	17
	2		21
4	6	11	19
	11		23
6	14	13	30
	9		26
7	10	15	29
	15		25

The cores listed contained the following elements:

Percentage of total sample

>.01	.01 to 1.00	1.00 to 10.00	<10.00
Cu	Cu	Mg	Ca
Ag	Mg	Si	
Ti	Si	Fe	
	Fe		
	V		
	Sr		
	Al		
	Mn		

C—Results of Iron Content Analyses

The values listed are the average of two determinations in most cases.

Core pair	Core	Average percent of total sample
1	1	.421 T
	2	.355 B
2	5	.599 T
	4	.320 B
3	3	.466 T
	7	.397 B
4	6	.362 T
	11	.387 B
5	8	.523 T
	13	.352 B
6	14	.453 T
	9	.416 B
7	10	.630 T
	15	.341 B
8	12	.540 T
	16	.423 B
9	17	.488 T
	21	.353 B
10	22	.506 T
	18	.339 B
11	19	.564 T
	23	.386 B
12	24	.577 T
	20	.401 B
13	30	.389 T
	26	.416 B
14	27	.439 T
	28	.338 B
15	29	.522 T
	25	.438 B

D—Results of Insoluble Residue Analyses

Insolubles were run on 16 of the cores or eight of the core pairs of the block. Approximately 1 gram samples of finer than 200-mesh powder were digested in commercial hydrochloric acid. Residues were carefully washed, dried, and weighed.

Core pair	Core	Weight sample before acid, mg	Weight sample after acid, mg	Percent insoluble
1	1 T	1000	135	13.5
	2 B	1016	134	13.2
3	3 T	1048	88	8.3
	7 B	1016	115	11.3
6	14 T	993	136	13.7
	9 B	1123	153	13.6
8	12 T	1053	122	11.5
	16 B	1022	115	11.2
11	19 T	1006	160	15.9
	23 B	1150	143	12.4
12	24 T	900	102	11.3
	20 B	1079	79	7.3
13	30 T	1001	129	12.7
	26 B	1017	121	11.1
14	27 T	1000	112	11.2
	28 B	998	131	13.3

E—Normal Atmosphere Artificial Glow Curve Peak Heights

These peak heights are computed, equated values. Each original peak height (centimeters) was multiplied by the correct radiation dosage factor listed in Appendix A. The result was multiplied by the correct amplification factor. The final values for each peak are listed below.

peak 1

Core pair	Core	Fraction *a*	Fraction *b*	Fraction *c*	Disks
1	1	16.4 T	18.98 T	6.0 T	11.92 B
	2	23.3 B	27.01 B	5.56 B	
2	5	2.95 T	3.67 T	.57 T	17.99 B
	4	15.6 B	12.67 B	3.16 B	9.32 T
3	3	13.55 T	12.4 T	3.67 T	18.82 B
	7	25.0 B	17.33 B	3.91 B	5.4 T
4	6	17.25 T	16.95 T	6.75 T	11.57 B
	11	20.4 B	18.5 B	12.6 B	1.6 T
5	8	14.75 T	14.7 T	6.15 T	21.5 B
	13	17.8 B	19.2 B	7.6 B	16.84 T
6	14	6.1 T	6.03 T	2.3 T	19.86 B
	9	15.4 B	14.5 B	6.7 B	18.37 T
7	10	11.1 T	11.63 T	4.06 T	17.0 B
	15	16.65 B	19.75 B	5.1 B	2.8 T
8	12	3.2 T	3.2 T	1.07 T	14.5 B
	16	18.75 B	19.64 B	9.3 B	12.62 T
9	17	4.75 T	4.94 T	.83 T	5.6 B
	21	14.35 B	27.64 B	7.5 B	2.8 T
10	22	1.75 T	2.58 T	.96 T	16.92 B
	18	11.55 B	13.66 B	5.13 B	3.13 T
11	19	1.7 T	2.14 T	.66 T	2.96 B
	23	14.8 B	14.54 B	6.75 B	2.63 T
12	24	2.35 T	2.19 T	1.15 T	9.23 B
	20	13.9 B	11.52 B	5.02 B	1.65 T
13	30	4.25 T	7.24 T	.86 T	7.46 B
	26	21.8 B	19.53 B	11.44 B	5.65 T
14	27	6.15 T	5.7 T	1.97 T	27.64 B
	28	18.4 B	15.85 B	5.27 B	3.67 T
15	29	3.55 T	3.73 T	.29 T	17.69 B
	25	12.7 B	16.56 B	6.3 B	2.65 T

peak 2

Core pair	Core	Fraction *a*	Fraction *b*	Fraction *c*	Disks
1	1	1.5 T	1.7 T	.56 T	2.74 B
	2	2.18 B	2.32 B	.47 B	2.72 T
2	5		1.3 T		1.33 B
	4	1.69 B	1.6 B	.31 B	
3	3	1.28 T	1.2 T	.31 T	1.36 B
	7	2.18 B	1.48 B	.27 B	.33 T
4	6	1.5 T	1.5 T	.51 T	.93 B
	11	1.85 B	1.61 B	1.01 B	.23 T
5	8	1.7 T	1.69 T	.75 T	1.85 B
	13	1.65 B	1.66 B	.74 B	1.29 T
6	14	.94 T	.88 T	.34 T	1.48 B
	9	1.58 B	1.51 B	.66 B	1.45 T
7	10	1.44 T	1.45 T	.52 T	1.37 B
	15	1.36 B	1.84 B	.4 B	.38 T
8	12				1.4 B
	16	1.89 B	1.85 B	.77 B	1.46 T
9	17				.71 B
	21	1.39 B	2.5 B	.66 B	.40 T
10	22				1.63 B
	18	1.26 B	1.45 B	.52 B	.48 T
11	19				.50 B
	23	1.53 B	1.41 B	.59 B	
12	24				.86 B
	20	1.65 B	1.4 B	.52 B	.54 T
13	30				.81 B
	26	2.06 B	1.77 B	.92 B	.83 T
14	27	.71 T	.73 T	.23 T	2.03 B
	28	1.6 B	1.48 B	.47 B	.52 T
15	29				1.85 B
	25	1.44 B	1.69 B	.7 B	.42 T

peak 3

Core pair	Core	Fraction *a*	Fraction *b*	Fraction *c*	Disks
1	1				
	2				
2	5	1.08 T	1.3 T	.3 T	
	4				
3	3	1.49 T	1.43 T	.42 T	
	7				.81 T
4	6				
	11				.41 T
5	8	1.76 T	1.69 T	.74 T	
	13				
6	14	1.18 T	1.1 T	.45 T	
	9				
7	10	1.36 T	1.37 T	.51 T	
	15				.61 T
8	12	1.09 T	1.12 T	.47 T	
	16				1.55 T
9	17	1.14 T	1.04 T	.27 T	1.0 B
	21				.73 T
10	22	.71 T	.93 T	.37 T	
	18				.82 T
11	19	.71 T	.88 T	.30 T	.70 B
	23				.96 T
12	24	.99 T	.92 T	.41 T	
	20				.54 T
13	30	1.0 T	1.29 T	.29 T	
	26				
14	27	1.09 T	1.11 T	.38 T	
	28				1.06 T
15	29	1.1 T	1.1 T	.3 T	1.14 B
	25	1.6 B	1.8 B	.77 B	.75 T

peak 4

Core pair	Core	Fraction *a*	Fraction *b*	Fraction *c*	Disks
1	1	2.2 T	2.4 T	.56 T	4.53 B
	2	2.84 B	2.73 B	.84 B	4.07 T
2	5	.76 T	.92 T	.28 T	2.24 B
	4	2.84 B	2.37 B	.79 B	1.26 T
3	3	1.99 T	1.85 T	.61 T	2.05 B
	7	3.28 B	2.36 B	.78 B	.83 T
4	6	2.51 T	2.25 T	.82 T	2.5 B
	11	2.31 B	2.04 B	1.08 B	.37 T
5	8	2.05 T	1.7 T	.74 T	2.29 B
	13	2.75 B	2.58 B	1.18 B	2.08 T
6	14	1.28 T	1.11 T	.49 T	2.26 B
	9	2.38 B	2.19 B	.96 B	2.14 T
7	10	1.48 T	1.44 T	.50 T	1.7 B
	15	2.38 B	2.82 B	.90 B	.72 T
8	12	.96 T	.95 T	.35 T	2.21 B
	16	2.59 B	2.32 B	1.11 B	.25 T
9	17	1.04 T	.95 T	.32 T	1.14 B
	21	1.99 B	2.8 B	.97 B	.83 T
10	22	.7 T	.84 T	.37 T	2.32 B
	18	2.25 B	2.3 B	.87 B	.91 T
11	19	.58 T	.66 T	.24 T	.70 B
	23	2.33 B	2.02 B	.84 B	1.13 T
12	24	.78 T	.75 T	.37 T	1.56 B
	20	2.26 B	1.86 B	.73 B	.49 T
13	30	1.0 T	1.15 T	.38 T	1.89 B
	26	3.2 B	2.74 B	.38 B	1.49 T
14	27	1.33 T	1.3 T	.46 T	2.96 B
	28	2.93 B	2.44 B	.88 B	1.44 T
15	29	1.0 T	.97 T	.37 T	2.03 B
	25	1.9 B	2.06 B	.80 B	.61 T

F—Nitrogen Atmosphere Artificial Glow Curve Peak Heights

These peak heights are computed, equated values of nitrogen atmosphere artificial glow curves using the intermediate or *b* fraction. Each original peak height in centimeters was multiplied by the correct radiation dosage factor listed in Appendix A. The resulting answer was multiplied by the correct amplification factor. The final values for each peak are listed below.

Core pair	Core	Peak 1N	Peak 2N	Peak 3N	Peak 4N
1	1	9.98 T	1.7 T		2.33 T
	2	14.81 B	2.22 B		2.63 B
2	5	1.76 T		1.43 T	.88 T
	4	7.24 B	1.70 B		2.58 B
3	3	7.46 T	1.37 T	1.48 T	1.95 T
	7	10.75 B	1.78 B		2.72 B
4	6	10.53 T	1.76 T		2.63 T
	11	11.41 B	1.84 B		2.30 B
5	8	8.56 T	1.92 T	1.91 T	2.17 T
	13	13.27 B	2.22 B		3.46 B
6	14	3.29 T	.93 T	1.13 T	1.28 T
	9	8.94 B	1.62 B		2.38 B
7	10	7.68 T	1.84 T	1.54 T	1.65 T
	15	12.83 B	2.32 B		3.1 B
8	12	1.76 T		1.21 T	1.06 T
	16	12.83 B	2.1 B		2.66 B
9	17	2.52 T		1.32 T	1.17 T
	21	19.42 B	3.16 B		3.29 B
10	22	1.32 T		1.04 T	.93 T
	18	8.78 B	1.7 B		2.55 B
11	19	1.097 T		1.097 T	.77 T
	23	9.87 B	1.78 B		2.36 B
12	24	.99 T		.98 T	.72 T
	20	6.97 B	1.56 B		2.09 B
13	30	3.29 T		1.37 T	1.15 T
	26	12.08 B	1.98 B		2.91 B
14	27	3.4 T	.92 T	1.25 T	1.42 T
	28	13.71 B	1.92 B		2.94 B
15	29	1.76 T		1.13 T	.99 T
	25	9.38 B	1.98 B	1.98 B	2.3 B

G—Natural Glow Curve Peak Heights

These peak heights are the actual measurements of the high-temperature peak in centimeters. The *b* fraction was used.

Core pair	Core	Peak height
1	1	7.8 T
	2	6.35 B
2	5	3.0 T
	4	7.65 B
3	3	7.45 T
	7	10.3 B
4	6	7.6 T
	11	5.8 B
5	8	9.3 T
	13	11.4 B
6	14	4.8 T
	9	7.0 B
7	10	5.5 T
	15	9.8 B
8	12	4.5 T
	16	7.2 B
9	17	
	21	6.9 B
10	22	4.1 T
	18	8.5 B
11	19	2.5 T
	23	6.0 B
12	24	3.05 T
	20	4.45 B
13	30	4.4 T
	26	9.6 B
14	27	5.6 T
	28	10.5 B
15	29	
	25	8.15 B

REFERENCES

Angino, E. E., 1958, Pressure-induced thermoluminescence as a geological age determination method: Unpub. master's thesis, Kansas Univ.

————, 1959, Pressure effects on thermoluminescence of limestone relative to geologic age: Jour. Geophys. Research, v. 64, no. 5, p. 569-573.

Bergstrom, R. E., 1956, Surface correlation of some Pennsylvanian limestones in the Mid-continent by thermoluminescence: Am. Assoc. Petroleum Geologists Bull., v. 40, p. 918-942.

Medlin, W. L., 1959, Thermoluminescent properties of calcite: Jour. Chem. Phys., v. 30, p. 451-458.

Parks, J. M., 1953, Use of thermoluminescence of limestone in subsurface stratigraphy: Am. Assoc. Petroleum Geologists Bull., v. 37, p. 125-142.

Pearn, W. O., 1959, Thermoluminescence applied to the dating of certain tectonic events: Unpub. master's thesis, Kansas Univ.

Pitrat, C. W., 1956, Thermoluminescence of limestone of Mississippian Madison Group in Montana and Utah: Am. Assoc. Petroleum Geologists Bull., v. 40, p. 943-952.

Saunders, D. F., 1953, Thermoluminescence and surface correlation of limestones: Am. Assoc. Petroleum Geologists Bull., v. 37, p. 114-124.

Zeller, E. J., 1953, Thermoluminescence of artificially precipitated calcite [*abs.*]: Geol. Soc. America Bull., v. 64, p. 1496-1497.

————, 1954a, Thermoluminescence of carbonate sediments, *in* Nuclear geology, H. Foul, ed.: John Wiley and Sons, New York, p. 180-188.

————, 1954b, Thermoluminescence as a radiation damage method of geologic age determination: 19th Internat. Geol. Cong., Algers 1952, sec. 12, p. 365-373.

————, and Ronca, L. B., 1962, New developments in the thermoluminescence method of geologic age determination: [presented at Symposium on Radioactive Dating, Athens, Greece, 1962] Kansas Univ. Press, Lawrence, 14 p.

————, Wray, J. L., and Daniels, F., 1955, Thermoluminescence induced by pressure and by crystallization: Jour. Chem. Phys., v. 23, p. 2187.

————, ————, ————, 1957, Factors in age determinations of carbonate sediments by thermoluminescence: Am. Assoc. Petroleum Geologists Bull., v. 41, p. 121-129.

BULLETIN 165 **1963 REPORTS OF STUDIES**

Part 1. **Preliminary Report on Conodonts of the Meramecian Stage (Upper Mississippian) from the Subsurface of Western Kansas,** by Thomas L. Thompson and Edwin D. Goebel, p. 1-16, fig. 1-3, August, 1963.

Part 2. **Sources of Error in Thermoluminescence Studies,** by Jesse M. McNellis, p. 1-23, fig. 1-26, December, 1963.